DTU Library

Synthesis and characterization of iron-cobalt (FeCo) alloy nanoparticles supported on carbon

Koutsopoulos, Sotiris; Barfod, Rasmus; Eriksen, Kim Michael; Fehrmann, Rasmus

Synthesis and characterization of iron-cobalt (FeCo) alloy nanoparticles supported on carbon

Sotirios Koutsopoulos [a,*], Rasmus Barfod [a], Dimitris Tsamouras [b], K. Michael Eriksen [a] and Rasmus Fehrmann [a]

[a] Department of Chemistry and Centre for Catalysis and Sustainable Chemistry, Building 206, Technical University of Denmark, DK-2800, Lyngby, Denmark and [b] Department for Polymer Chemistry and Materials Science Center, University of Groningen, Nijenborgh 4, 9747, AG Groningen, The Netherlands.

* Corresponding author's present address: Center for Biomedical Engineering, Massachusetts Institute of Technology, NE47-378, Cambridge, MA 02139-4307, USA, Tel: +1-617-752-2042, Email: sotiris@mit.edu

ABSTRACT

Iron-cobalt nanocrystaline bimetallic alloys supported on carbon microparticles were synthesized and characterized. The preparation methods involved the use of iron and cobalt chloride or acetate precursor salts in water and direct co-precipitation or wet impregnation techniques. The size of the alloy nanoparticles differed depending on the preparation method. When the wet impregnation technique of acetate precursor salts of Fe and Co were used for the synthesis, the size of FeCo alloy nanoparticles was approximately 13 nm. FeCo alloy nanoparticles were characterized by crystallography (XRD), thermogravimetric analysis (TGA), electron microscopy, energy dispersive X-ray spectroscopy analysis (EDX), and atomic force microscopy (AFM). In all cases, we observed well-dispersed nanometer size alloy particles on the surface of carbon microparticles. FeCo supported on such carbon microparticles are chemically and mechanically stable for prolonged periods of time. AFM analysis showed that the FeCo nanoparticles were formed on the surface of the carrier. The results of this study suggest that using these easy and inexpensive synthetic methods iron-cobalt nanoparticles can be formed on carbon microparticles support materials with applications in catalysis, microelectronics, and biomedicine.

INTRODUCTION

The synthesis of nanoparticles with controlled size and composition is of fundamental scientific and technological interest. Nanosized particles exhibit different, often enhanced, magnetic, electronic, optical, and reactive properties compared to the corresponding bulk materials making them desirable for applications in catalysis, electronics, and biomedicine [1,2,3,4,5,6]. In many applications, transition metals provide a distinct advantage over precious metals due to their lower cost and availability. Interest in iron-containing nanoparticles originates primarily from the metal's magnetic and electronic properties, its availability and low cost, and its high reactivity in reducing atmospheres [1,3]. Notable applications of iron nanoparticles are in the field of catalysis for the Fischer-Tropsch reaction, the synthesis of ammonia, the reduction of oxygen in fuel cells, and CO oxidation [3,7,8,9].

Almost all alloying additions decrease the saturation magnetization of iron except for cobalt and manganese [10,11,12]. FeCo bimetallic alloys exhibit high saturation magnetization, which is due to the increased polarization of Fe atoms in the presence of Co [13,14], and the high Curie temperature (i.e., 900°C) [12,15,16]. Alloy-based ferromagnetic nanoparticles supported on an insulating or conducting carrier are of great importance because they exhibit unusual magnetic properties which are dependent on the size of the magnetic nanoparticles, their chemical composition and the interparticle magnetic interactions [17]. In catalysis, the addition of Co to Fe-based catalysts results in a more active catalyst for NH_3 synthesis [18]. FeCo alloy nanoparticles supported on diverse carriers are of great interest due to their properties in catalysis including the synthesis of ammonia and the fabrication of carbon nanotubes which have numerous applications in nanotechnology [19,20]. The synthesis and dispersion of FeCo alloy nanoparticles on the support material results in: (i) increased stability and mechanical properties of the final product (ii) higher exposed surface area of the FeCo nanoparticles resulting in increased surface to volume ratio of the active metals, and (iii) narrow size distribution compared with preparations of unsupported metals or alloys.

Carbon microparticles are suitable support materials because they have high specific surface area, are resistant to acidic and basic conditions, provide metal loading sites on the particle surface, are stable at high temperatures in anoxic conditions, and do not allow electron delocalization on the carbon surface which is important in catalysis and electronics [21]. Furthermore, carbon-based materials are low cost and amenable to chemical and structural modifications to modulate through non-covalent and covalent methods their chemical, electronic, and crystalline properties. This allows for the design of tailor-made catalytical

materials and electrochemical devices including sensors, lithium-ion batteries, and super-capacitors [22,23,24]. FeCo nanoparticles supported on carbon microparticles have potential applications in catalysis for the synthesis ammonia, as magnetic materials in data storage devices, in the development of advanced microelectronics, and in biomedicine as contrasting agents for the detection of tumors using magnetic resonance imaging (MRI) and in photothermal-ablation therapeutics [25,26,27,28]. Notably, preformed FeCo alloy nanoparticles with magnetic properties embedded in a carbon matrix are suitable precursor materials for the synthesis of carbon-based FeCo nanohybrid systems [29]. Such materials have important applications in data storage devices because it has been predicted for FeCo nanoparticles may be stabilized upon alloying with carbon [30].

In this paper, we investigated the synthesis of FeCo bimetallic alloy nanoparticles supported on carbon microparticles that are characterized by high specific surface area and inertness. We aimed at producing these materials using an inexpensive and fast method and therefore, for the synthesis, we used co-precipitation and wet impregnation of the carbon microparticles with the respective metal's precursor salts. Both of these techniques are commonly used for the synthesis of metal nanoparticles supported on support materials. The synthetic strategy and the choice of the precursor salts offer allow for control of the particle formation and the composition of the FeCo alloy nanoparticles in the final sample [31,32,33]. The resulting products were characterized by X-ray powder diffraction (XRD), transmission electron microscopy (TEM), energy dispersive X-ray spectroscopy analysis (EDX), and atomic force microscopy (AFM). The results showed that the preparation methods that were used allow for the synthesis of FeCo nanoparticles with narrow size distribution and the desired Fe:Co ratio supported on the surface grooves of the carbon microparticles.

EXPERIMENTAL

Materials and chemicals

Carbon-black powder microparticles Vulcan® XC72R were used to support FeCo alloy nanoparticles. The carbon material has a specific surface area of ca. 190 m^2/g and consists of aggregates of nanoparticles each having an average diameter of about 35 nm. Direct co-precipitation and wet impregnation were used to prepare the carbon-supported FeCo alloy nanoparticles. $FeCl_2·4H_2O$ and $CoCl_2·6H_2O$ (Sigma-Aldrich) were used as precursor compounds when the direct co-precipitation method was employed whereas $Fe(CH_3COO)_2$ and

$Co(CH_3COO)_2 \cdot 4\ H_2O$ salts (Sigma-Aldrich) were used for the wet impregnation technique. Millipore water (Millipore, Bedford, MA) was used for the syntheses.

Synthesis of FeCo bimetallic alloys by direct co-precipitation

The synthesis was carried out under nitrogen gas flow. 4 mg of carbon particles were suspended in 200 ml deionized water, ultrasonicated, and equilibrated at 50°C for 3 hours and at 80°C for 1 hour under continuous stirring to increase the wettablity of the relatively hydrophobic surface of carbon (Figure 1). We aimed to prepare a sample with Fe:Co stoichiometry of 9:1 and metal loading of 15 %. Therefore, $26.71 \cdot 10^{-3}$ M $FeCl_2 \cdot 4H_2O$ and $2.97 \cdot 10^{-3}$ M $CoCl_2 \cdot 6H_2O$ (Sigma-Aldrich) in water were added to the carbon microparticle suspension to a final volume of 300 ml. The final solution was split in two portions and the pH of the suspension was adjusted to 9.2 using NH_3 or NaOH resulting in precipitation of the metal oxides. The two suspensions were allowed to equilibrate for 30 min at 50°C and for 10 min at 80°C. Then the carbon microparticles carrying the Fe and Co precipitates were filtered, washed with water to remove the supernatant which contains chloride ions, and dried in a vacuum oven overnight at 50°C.

The dried solid oxides were reduced under formier gas (i.e., mixture of $N_2:H_2$ with ratio 9:1) for 4 hours. Preliminary experiments were performed to determine the optimal temperature for complete reduction of the precipitated salts. In the case that NH_3 was used to adjust the pH, the reduction was complete upon heating at 400°C whereas in the case that Na^+ ions were introduced in the system reduction of the metal oxides required a heating step at 500°C for the complete reduction of the precipitated oxides to the metals. To avoid sintering of the particles the reduction was performed at the lowest temperature required to have complete reduction of the oxides. Prior to further characterization, the reduced samples were passivated by 2% gas mixture of O_2/N_2 for 30 min at room temperature.

Synthesis of FeCo bimetallic alloys by wet impregnation

When the impregnation technique was used, the acetate salts of Fe(II) and Co(II) were used as precursors (Figure 1). Both salts are very soluble in water and therefore, highly concentrated solutions could be prepared to increase the metal loading of the final product. Nitrate salts of Fe and Co were not considered due to their explosive properties. 1.65 g of $Fe(CH_3COO)_2$ and 0.28 g of $Co(CH_3COO)_2 \cdot 4\ H_2O$ (Sigma-Aldrich) were dissolved in 200 ml deionized water and the pH was adjusted to 6.5. These concentrations were chosen so that the alloy would have a Fe:Co stoichiometry of 9:1 and the metal loading of the final product would

be ca. 15 %. Then 4 g of heat treated carbon microparticles were added to the solution. The slurry was ultrasonicated for 20 min and equilibrated for 2 days under N_2 while the pH was maintained at 6-7. Then the solvent was evaporated slowly over a period of 20 hours at 45°C. After impregnation the samples were dried at 110°C overnight. The reduction process was performed under N_2:H_2 gas mixture with ratio 9:1 and involved 30 min step-heating of the samples at 100°C, 300°C, 400°C, and for 2.5 hours at 500°C, respectively. After reduction, the samples were passivated by 2% O_2/N_2 gas mixture for 30 min at room temperature.

Sample characterization

Thermogravimetric/differential thermal analysis (TGA-DTA) was used to determine the optimal temperature for reduction. During the analysis, the composition of the gas outlet was monitored by a mass spectrometer (MS) which was connected to the TGA-DTA setup. TGA-DTA temperature-programmed reduction experiments were carried out in a TGA cell (Mettler-Toledo). Before the measurements, all samples were pretreated for 2 hours at 200°C under N_2 gas flow to remove surface absorbed species. Subsequently, the sample was cooled to room temperature and the temperature increased in steps of 50°C for 30 min at each temperature up to 600°C under N_2:H_2 gas mixture with 9:1 ratio and gas flow of 110 ml/min.

XRD analysis was performed on an X-ray diffractometer (Philips PC-APD, $2\theta = 40 - 120°$, step size 0.02°) using Cu Kα radiation ($\alpha_1 = 1.5406$ Å, $\alpha_2 = 1.5444$ Å). The recorded diffraction patterns of two different preparations were analyzed to determine the crystallographic characteristics of the final product.

Microscopic examination of the samples was performed by TEM (Philips EM 430). A portion of the sample was ground in a mortar, suspended in ethanol, and dispersed by ultrasonication. A drop of the suspension was allowed to evaporate on a copper grid. Electron microscope pictures were taken at magnifications between 122,000x and 200,000x. From the TEM pictures the average size of the particles was determined (at least 80 particles from different TEM pictures were measured) using image analysis software. The dimensions of the particles were then averaged and the standard deviation was calculated. The quality of the images was poor due to the carbon material used in the synthesis. To distinguish individual FeCo nanoparticles for size determination, the brightness/contrast was adjusted for the entire image or locally, in specific locations in the image. The electron microscope was calibrated with an internal standard of asbestos to avoid the common source of error where the display magnification is higher than the correct value and the particles appear smaller. EDX was also performed to obtain information on the composition ratio of the chemical species in the imaged

areas. Atomic absorption spectroscopy (AAS) of samples suspended in acidic medium to dissolve the alloy particles was used to determine the metal ratio and compare the with the EDX results.

AFM studies of the sample surfaces were performed using a Nanoscope III multimode scanning probe microscope (Digital Instruments, Santa Barbara, CA) operated in tapping mode. The probe was a single-crystal silicon tip with a nominal curvature of < 10 nm which was mounted on a single-beam cantilever. Phase imaging was performed at 1 Hz and 512 samples per line. AFM images of the alloy crystals supported on the carbon surface were recorded in air at room temperature and at random spot sampling on the surface. For the determination of the diameter of the crystals the horizontal size of at least 80 particles on the surface were measured and averaged.

RESULTS AND DISCUSSION

To synthesize FeCo alloy nanoparticles on the high surface area carbon microparticles we used the direct co-precipitation and wet impregnation methods and the chloride or acetate salts of the metals as precursor compounds. Reduction of the carbon-supported precursor compounds is a critical step in the process which requires heating at elevated temperatures and often results in undesirable sintering of the nanoparticles. To determine the optimal temperature for reduction of the Fe and Co precipitated salts we used XRD analysis and mass spectrometry (MS) connected to a TGA-DTA instrument. Reduction was carried out in N_2:H_2 ratio 9:1 gas and the temperature for reduction was set to 400°C or 500°C depending on the sample preparation method. Post-treatment, the samples were cooled to room temperature slowly to avoid the formation of lattice defects in the FeCo nanoparticles. Our experiments showed that carbon microparticles decompose between 450°C and 500°C under air or oxygen but are stable under nitrogen atmosphere which was used for reduction.

To confirm that the reduction process was complete, the post-reduction samples were examined by XRD. We did not observe peaks that could be assigned to unreduced Fe and Co precursor oxides (JCPDS card no. 22-1086, 33-0664, 3-0864, 26-1136, 75-0419, 30-0443), Fe and Co acetates (CCDC No. 747548, and JCPDS card no. 22-1080, 29-465, 25-372) which were used in wet impregnation synthesis, or to non-alloyed Fe (JCPDS card no. 6-696 bcc phase) and Co (JCPDS card no. 5-0727 hcp phase and 15-0806 fcc phase) metals. Completion

of the reduction reaction was also manifested by MS of the reduction gas outlet which showed the absence of significant changes in the composition of the chemical species upon interaction of the reduction gas with the sample. In the analysis, we monitored CH_4, H_2O, H_2S, HCl, and CO_2 which are major components of the precursor salts or are involved in the reactions occurring during the reduction.

Synthesis of FeCo alloy nanoparticles by co-precipitation

To synthesize the FeCo alloy on Vulcan XC72 carbon microparticles, we first used the direct co-precipitation method of the Fe and Co chloride precursor salts. This method was chosen for its simplicity and the low-cost of the reagents which are important factors in industrial applications. The alloy composition is adjusted by controlling the molar ratio of the iron to cobalt precursor salts. When the co-precipitation method was used to synthesize the FeCo bimetallic alloy nanoparticels, the pH was adjusted to 9.2 by addition of NH_3 or NaOH, because in alkaline pH the solubility of iron and cobalt hydroxides is very low and therefore, almost all metal ions in the solution precipitate. The solubility products of both Fe and Co hydroxides are of the same order and therefore, it was assumed that both metal hydroxide compounds precipitate at a similar rate. AAS spectroscopy analyses showed that the FeCo loading was 14.1 wt% and 14.3 wt% when NH_3 or NaOH was used in the synthesis, respectively. These metal loadings are close to the desired loading of 15 wt% and confirm that almost all the Fe and Co ions precipitated on the surface of carbon. Furthermore, EDX analysis of more than 20 alloy nanoparticles supported on carbon showed that the Fe:Co ratio was 8.7:1.1 in both cases of NH_3 or NaOH used for the synthesis. This result suggests that the co-precipitation method results in the FeCo nanoparticles with a Fe:Co ratio that deviates from the stoichiometric ratio of the precursor salts which was adjusted to 9:1. However, the ease of the method allows for fine tuning adjustment of the final metal-to-metal ratio to the desired value simply by changing the ratio of the precursor salts concentrations in the precipitating medium.

XRD analysis of the post-reduction samples and temperature-programmed reduction measurements showed that reduction of the Fe and Co oxides was complete at 400°C when NH_3 was used to adjust the pH of the precipitating solution (Figure 2). In the case of NaOH used for the adjustment of the pH to 9.2, we observed that the reduction was not complete at 400°C but required another heating step at 500°C before the metal oxide peaks disappeared in the XRD spectra of the samples (Figure 3). The difference in the temperature for complete reduction of the two samples suggests that Na^+ ions may be incorporated in the alloy leading to the formation of Na-doped FeCo alloy nanoparticles.

Upon complete reduction of the Fe and Co precipitated salts, analysis of the diffraction patterns demonstrated the formation of the FeCo alloy with the characteristic reflections of the body centered cubic (bcc) phase (JCPDS card No. 48-1818, 49-1567, and 49-1568). The peaks at $2\theta°$ values of 44.52°, 64.75°, 82.16°, and 99.04° correspond to the crystal planes of (110), (200), (211), and (220), respectively of the crystalline FeCo alloy. Figures 2 and 3, show that after complete reduction of the precipitates at 400°C or 500°C when NH_3 or NaOH was used for the adjustment of pH, respectively, the diffraction pattern did not contain peaks that could be assigned to the Fe and/or Co oxides or to the pure Fe and Co metals. These results are in line with the XRD patterns of FeCo nanoparticles formed on the surface of Al_2O_3 [34] or graphitic carbon that was produced via an IR-heating route of polyacrylonitrile [35].

The FeCo lattice parameter was calculated from the XRD pattern refinement from two different syntheses for each condition and gave values of 0.2874 ± 0.0004 nm for FeCo prepared using either NH_3 or NaOH for the adjustment of pH. This value is higher than the cell constant of pure α-Fe (0.2867 nm) and similar to the value calculated for a $Fe_{8.8}Co_{1.2}$ alloy (0.2875 nm) prepared by mechanical alloying of the elemental powders using ball milling [36].

Peak width analysis was performed to calculate the average sizes of the FeCo alloy nanoparticles. Using the Debye-Scherrer formula on the full width at half-maximum (FWHM) of the (110) diffraction peak, we calculated that the diameter of the nanoparticles was 21.4 ± 2.2 nm and 22.7 ± 3.6 nm when NH_3 or NaOH was used in the synthesis, respectively. For the calculations we used diffraction patterns from two different preparations (n = 4).

The long-term stability of the samples in storage was also tested by comparing X-ray diffractograms that were obtained one week and four months after the syntheses. In all cases the diffractograms were indistinguishable suggesting the stability of the samples.

TEM image analysis of FeCo alloy nanoparticles formed on carbon microparticles showed that the nanoparticles were homogeneously distributed on the surface of carbon and that the average size of the FeCo nanoparticles is 22.8 ± 5.1 nm and 24.4 ± 4.8 nm when NH_3 or NaOH was used in the synthesis, respectively (Figure 4A and 4B). These values are similar with those obtained from the analysis of the X-ray diffraction peaks of the FeCo nanoparticles. The slightly larger nanoparticle size measured by TEM image analysis compared with that from the Debye-Scherrer formula, which usually underestimates the size of particles, is likely due to the fact that TEM provides the average projected diameter of nanoparticles which may overlap and are poorly resolved in the TEM images.

Synthesis of FeCo alloy nanoparticles by wet impregnation

We used the wet impregnation method to control the ratio of the precursor salt precipitates on the surface of the carbon microparticles. The rationale of using the acetate salts of the metals is that the precipitated bulky acetate crystals would result in small FeCo alloy particles after reduction and removal of the acetate groups. Temperature-controlled reduction of the precursor acetate salt precipitates with a gas mixture of $N_2:H_2$ ratio 9:1 was monitored by TGA-DTA/MS of the reactants outlet and showed that formation of the FeCo alloy was complete at 500°C (Figure 5). Monitoring the CO_2 that evolved during reduction also revealed useful information about the decomposition of the precursor acetate salts. Thermogravimetric analysis showed two CO_2 peaks. There was a strong peak at 260°C – 290°C and a smaller peak at 320°C – 340°C. These two peaks were previously ascribed to the heat-induced decomposition of $Fe(CH_3COO)_2$ followed by the subsequent release of CO_2 and it was suggested that 450°C is sufficient temperature for the reduction of $Fe(CH_3COO)_2$ [37,38]. In a previous study, formation of Co metal from decomposition of $Co(CH_3COO)_2$ in H_2 atmosphere was completed below 300°C [39]. From the TGA-DTA/MS experiments it is suggested that the alloy is formed through a mechanism that involves initially the removal of adsorbed water molecules at ca. 100°C, decomposition of the acetate salts and release of CO_2 and H_2O at ca. 300°C resulting in the formation of the metal oxides. The oxides were subsequently reduced between 300°C and 500°C to form the FeCo alloy. This was manifested by the release of H_2O (Figure 5).

XRD analysis confirmed that the post-reduction sample was characterized by diffraction peaks assigned to the FeCo alloy only formed on the surface of carbon. Peaks that could be assigned to Fe or Co oxides or to pure Fe or Co metals were not observed (Figure 6). Similar results were obtained for FeCo nanoparticles formed on the surface of Al_2O_3 [34]. Peak width analysis was used to calculate the average size of the FeCo nanoparticles using the Debye-Scherrer formula and we found that the diameter of the nanoparticles was 13.9 ± 4.7 nm (two preparations, n = 4).

Lattice parameter calculation of FeCo prepared by wet impregnation of the acetate precursors was found to be 0.2871 ± 0.0001 nm. X-ray analysis also showed that passivation of the FeCo alloy nanoparticles with 2% O_2/N_2 at room temperature for 30 min resulted in the formation of the metal oxides on the surface of the alloy nanoparticles (Figure 6). Formation of Fe and Co oxides upon passivation was negligible when the direct co-precipitation synthesis method was used (Figures 2 and 3). This result suggests that the size of the nanoparticles is an important factor in determining the stability of the FeCo nanoparticles in air and that nanoparticles with sizes ~ 13 nm are more susceptible to oxidation compared to the 21-23 nm nanoparticles that were obtained by the co-precipitation method. Further reduction of the

passivated FeCo nanoparticles at 400°C followed by XRD examination showed that the metal oxide diffraction peaks were not present. This diffractogram was identical to that obtained for the same sample prior to passivation and TEM images did not show the typical gray shell indicative of metal oxides on the surface of the alloy nanoparticles. Metal oxides have lower electron density than the metallic FeCo core and therefore they would look much lighter. This suggests that oxidation occurred only on a thin layer on the surface of the nanoparticles. XRD peak analysis of the samples one week and four months after the synthesis showed that the samples were stable in storage during this period of time.

In agreement with the diffraction peak analysis, TEM image analysis showed that the average size of the bimetallic alloy nanoparticles is about 13.3 ± 3.5 nm (Figure 4C) which is similar with that observed using the X-ray peak analysis. The calculations of the size of the FeCo alloy nanoparticle revealed another interesting point. FeCo nanoparticles obtained using the metal acetate precursor salts and the wet impregnation technique are smaller than the superparamagnetic size limit of ca. 20 nm which was calculated by using the low magnetic anisotropy of FeCo [40,41,42] suggesting that the FeCo nanoparticles produced by this method may have superparamagnetic properties. Further work will be required to confirm this assumption.

EDX analysis of the alloy nanoparticles supported on carbon showed that the Fe:Co ratio of the alloy was 9:1 which is identical to the reactants ratio suggesting that wet impregnation offers good control of the metal ratio. Furthermore, AAS quantitative analyses showed that the FeCo loading on the surface of carbon was ca. 15%.

AFM imaging

FeCo alloy nanoparticles supported on the surface of carbon were visualized by AFM phase imaging in which the phase shift of the oscillating cantilever was measured relative to the driving signal. This phase shift was correlated with specific mechanical, friction, adhesion, or viscoelasticity properties of the material that affect the tip-sample interaction [43]. We used phase imaging because standard height surface analysis resulted in poor quality images. Phase imaging provided surface images with nanometer resolution. Based on the AFM images, FeCo nanoparticles appear to be well distributed on the surface of the carbon (Figure 7, right panel). Furthermore, phase contrast AFM allowed for distinguishing materials with different mechanical properties like carbon and the metal alloy [43]. We found that the FeCo nanoparticles were preferentially formed at the interface between carbon nanoparticle aggregates which form the carbon microparticles and had an average size of 12.0 ± 0.3 nm. This is in agreement with the

TEM image analysis and XRD peak processing using the Debye-Scherrer equation. The average diameter of the carbon nanoparticles was calculated to be ca. 35 nm which is in agreement with the manufacturer's material specifications.

CONCLUSIONS

In this work, we used the direct co-precipitation and wet impregnation methods of the metal precursor salts to synthesize FeCo alloy nanoparticles supported on carbon. The synthetic methods that were used are suitable for controlling the alloy composition in the final product by changing the ratio of the concentration of the precursor salts. In the case of co-precipitation of the metal oxides, formation of the alloy upon reduction of the oxides was completed at a significantly lower temperature (i.e., 400°C) when NH_3 was used to adjust the pH compared with the temperature that was necessary for complete reduction (i.e., 500°C) when NaOH was used to adjust the pH. Formation of the alloy was confirmed by X-ray analysis while TEM and AFM were used to obtain images of the nanoparticles on the surface of carbon. Using AFM, we obtained a representation of the surface of the carbon in which the FeCo single crystals were nested at the interface of aggregated carbon nanoparticles. Using these simple synthetic methods we were able to produce FeCO bimetallic alloy nanoparticles of ca. 13 nm (in the case of wet impregnation of the metal acetate salts) and ca. 23 nm (in the case of co-precipitation of the metal oxides). Our also results showed that the smaller (i.e. 13 nm) FeCo nanoparticles are prone to oxidation upon sample passivation at room temperature whereas the larger nanoparticles produced by co-precipitation were resistant to oxidation at the same conditions. The synthesis of FeCo nanoparticles of such sizes has many potential applications in data storage devices, microelectronics, catalysis, and medicine.

References

[1] S. Enthaler, K. Junge, M. Beller, Angew. Chem. Int. Ed. 47 (2008) 3317–3321.

[2] A.N. Shipway, E. Katz, I. Willner, ChemPhysChem 1 (2000) 18–52.

[3] D.L. Huber, (2005) Small 1:482–501.

[4] D. Davidovic, M. Tinkham, Appl. Phys. Lett. 73 (1998) 3959-3961.

[5] S. Koutsopoulos, T. Johannessen, K.M. Eriksen, R. Fehrmann, J. Catal. 238 (2005) 206-213.

[6] T. Johannessen, S. Koutsopoulos, J. Catal. 205, (2002) 404-408.

[7] B.H. Davis, Catal. Today 84 (2003) 83–98.

[8] F. Jaouen, S. Marcotte, J.-P. Dodelet, G. Lindbergh, J. Phys. Chem. B 107 (2003) 1376–86.

[9] G. Bian, A. Oonuki, A. Kobayashi, N. Koizumi, M. Yamada, Appl. Catal. A Gen 219 (2001) 13–24.

[10] R.M. Bozorth, "Ferromagnetism" D. Van Nostrand Co. Inc. (1951)

[11] R.C. Hall, Trans. TMS-AIME 218 (1960) 268–270.

[12] R.S. Sundar, S.C. Deevi, Int. Mater. Rev. 50 (2005) 157–192.

[13] N. Hamada, J. Phys. Soc. Jpn. 46 (1979) 1759–1766.

[14] J.M. MacLaren, T.C. Schulthess, W.H. Butler, R. Sutton, M. McHenry, J. Appl. Phys. 85 (1999) 4833–4835.

[15] P. Weiss, Trans. Faraday Soc. 8 (1912) 149–156.

[16] P. Weiss, R. Forrer, Ann. Phys. (Paris) 12 (1929) 279–374.

[17] A. Falqui, V. Serin, L. Calmels, E. Snoeck, A. Corrias, G. Ennas, J. Microscopy, 210, (2003) 80-88.

[18] R.J. Kaleńczuk, Appl. Catal. A Gen 112 (1994) 149-160.

[19] D. Carta, F. Boi, A. Corrias, S. Bullita, Z. Kónya, M.F. Casula, J. Porous Mater., 21, (2014) 1123-1131.

[20] R.H. Baughman, A.A. Zakhidov, W.A. De Heer, Science, 297, (2002) 787-792.

[21] F. Rodriguez-Reinoso Carbon 36 (1998) 159–175.

[22] X. W. Mao, F. Simeon, G. C. Rutledge, T. A. Hatton, Adv Mater 2013, 25, 1309.

[23] D.Y. Pan, S. Wang, B. Zhao, M.H. Wu, H. J. Zhang, Y. Wang, et al., Chem Mater 2009, 21, 3136.

[24] Y.W. Zhu, S. Murali, M.D. Stoller, K.J. Ganesh, W.W. Cai, P.J. Ferreira, et al., Science 2011, 332, 1537

[25] K.E. Mooney, M.J. Wagner, J. Mater. Chem. 19 (2009) 611-616

[26] S. Hagen, R. Barfod, R. Fehrmann, C.J.H. Jacobsen, H.T. Teunissen, I. Chorkendorff, J. Catal. 214 (2003) 327-335

[27] W.S. Seo, J.H. Lee, X.M. Sun, Y. Suzuki, D. Mann, Z. Liu, M. Terashima, P.C. Yang, M.V. McConnell, D.G. Nishimura, H.J. Dai, Nature Mater. 5 (2006) 971-976

[28] V.V. Mody, M.I. Nounou, M. Bikram, Adv. Drug Del. Rev. 61 (2009) 795-807.

[29] G. Khadra, A. Tamion, F. Tournus, O. Boisron, C. Albin, V. Dupuis. Structure and Magnetic Properties of FeCo Clusters: Carbon Environment and Annealing Effects. J. Phys. Chem. C, 121(20), (2017) 10713-10718.

[30] E.K. Delczeg-Czirjak, A. Edström, M. Werwinski, J. Rusz, N.V. Skorodumova, L. Vitos, O. Eriksson. Stabilization of the Tetragonal Distortion of FexCo1−x Alloys by C Impurities: A Potential New Permanent Magnet. Phys. Rev. B: Condens. Matter Mater. Phys. 2014, 89, 144403−144407.

[31] S. Koutsopoulos, S.B. Rasmussen, SB K.M. Eriksen, R. Fehrmann, Appl. Catal. A – General 306 (2006) 142-148.

[32] S. Koutsopoulos, K.M. Eriksen, R. Fehrmann, J. Catal. 238 (2006) 270-276

[33] S. Koutsopoulos, T. Johannessen, K.M. Eriksen, R. Fehrmann, J. Catal. 238 (2006) 206-213

[34] A. Corrias, M.F. Casula, A. Falqui, G. Paschina, Chem. Mater., 16, (2004) 3130-3138.

[35] L.V. Kozhitov, M.F. Bulatov, V.V. Korovushkin, V.G. Kostishin, D.G. Muratov, M.N. Shipko, S.G. Emelyanov, E.V. Yakushko. The Formation and Study of the FeCo Nanoparticles Alloy in Structure of Metal-Carbon Nanocomposites FeCo/C. J. Nano- and Electronic Physics 7 (2015) 4103-4101.

[36] H. Moumeni, S. Alleg, C. Djebbari, F.Z. Bentayeb, J.M. Greneche, J. Mater. Sci. 39 (2004) 5441-5443.

[37] K. Ehrensberger, H.W. Schmalle, H.-R. Oswald, A. Reller, J. Therm. Anal. Calorim. 57 (1999) 139-149.

[38] J.C. Kuriacose, S.S. Jewur, J. Catal. 50 (1977) 330-341.

[39] M.A. Mohamed, S.A. Halawy, M.M. Ebrahim, J. Thermal Anal. 41 (1994) 387-404.

[40] D.I. Bardos, J. Appl. Phys. 40:1(1969) 371–1372.

[41] A. Hütten, D. Sudfeld, I. Ennen, G. Reiss, W. Hachmann, U. Heinzmann, K. Wojczykowski, P. Jutzi, W. Saikaly, G. Thomas, J. Biotechnol. 112 (2004) 47–63.

[42] G. Reiss, A. Hütten, Nature Mater. 4 (2005) 725–726.

[43] S.N. Magonov, V. Elings, M.-H. Whangbo, Surf. Sci. 375 (1997) L385-L391.

Table 1. Synthesis, properties and characterization of FeCo alloy nanoparticles on the carbon surface.

Precursor salts	Synthesis	Reduction temperature	Particle size (Debye-Scherrer)	Particle size (TEM imaging)
FeCl$_2$ / CoCl$_2$	co-precipitation of oxides using NH$_3$ to adjust pH to 9.2	400°C	21.4 ± 2.2 nm	22.8 ± 5.1 nm
FeCl$_2$ / CoCl$_2$	co-precipitation of oxides using NaOH to adjust pH to 9.2	500°C	22.7 ± 3.6 nm	24.4 ± 4.8 nm
Fe(CH$_3$COO)$_2$ / Co(CH$_3$COO)$_2$	wet impregnation	500°C	13.9 ± 4.7 nm	13.3 ± 3.5 nm

Legends to Figures

Figure 1   Synthetic pathways for the preparation of FeCo bimetallic alloy nanoparticles on carbon particles using the co-precipitation and wet-impregnation techniques.

Figure 2   X-ray diffraction pattern of the FeCo alloy nanoparticles supported on carbon after reduction at 400°C. For the synthesis, the direct co-precipitation method of the Fe and Co hydroxides was used and the pH was adjusted to 9.2 by addition of NH_3.

Figure 3   X-ray diffraction pattern of the FeCo alloy nanoparticles supported on carbon after reduction at 400°C and 500°C. For the preparation, the direct co-precipitation method of the Fe and Co hydroxides was used and the pH was adjusted to 9.2 by NaOH.

Figure 4   Typical TEM pictures of the FeCo alloy nanoparticles supported on carbon microparticles. (A and B) FeCo nanoparticles were formed by the direct precipitation method using the respective metal chloride precursor salts and the pH was adjusted to 9.2 by (A) NH_3 or (B) NaOH. (C) FeCo nanoparticles formed using the wet impregnation technique of the metal acetate precursor salts.

Figure 5   Decomposition of the $Fe(CH_3COO)_2$ and $Co(CH_3COO)_2$ precursor salts. TGA/MS graphs monitor the formation of the FeCo alloy supported on carbon microparticles using the wet impregnation technique.

Figure 6   X-ray diffraction patterns of the FeCo alloy on carbon after reduction at 500°C. The preparation method consisted of wet impregnation of the Fe(II) and Co(II) acetate precursor salts on the surface of carbon.

Figure 7   AFM phase imaging of FeCo alloy nanoparticles supported on carbon microparticles using the wet impregnation technique. The nanoparticles are formed on the surface of the carbon microparticles which consist of aggregates of carbon nanoparticles with average diameter of ca. 35 nm. Image analysis of the sample surface showed that the average diameter of the alloy nanoparticles is ca. 12 nm. Phase images were recorded at 1 Hz and 512 samples per line.
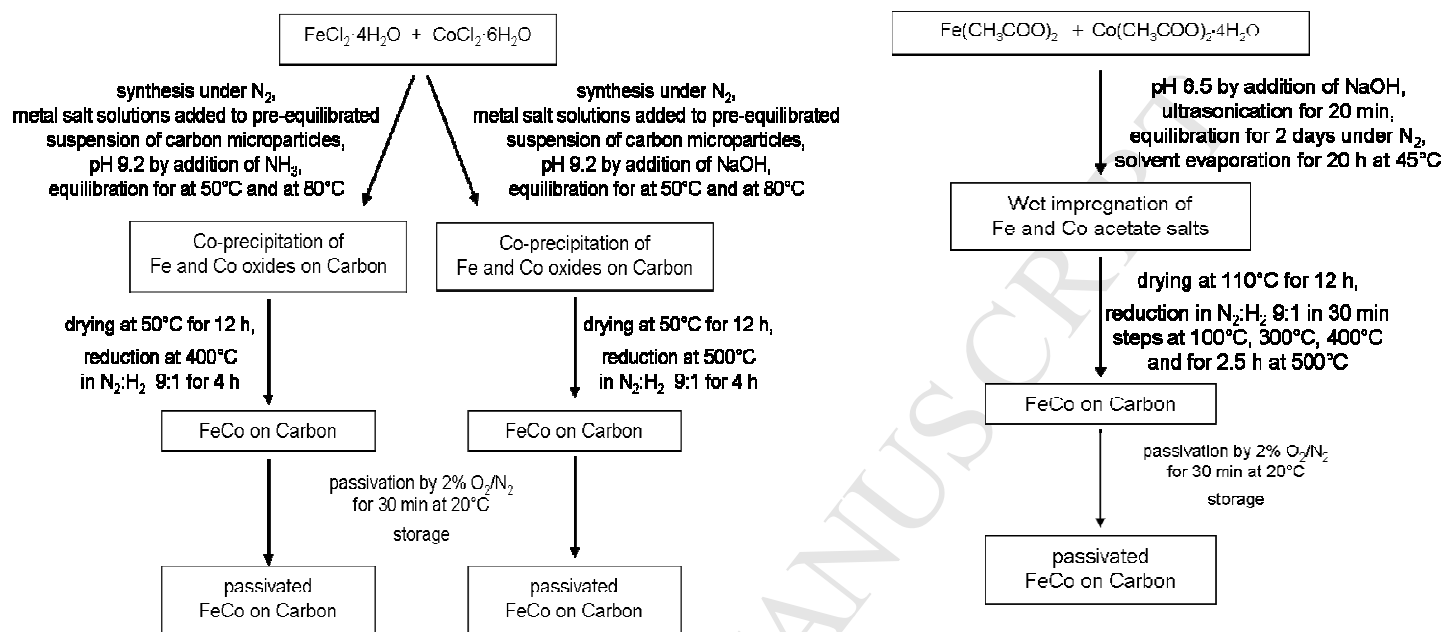
FeCl$_2$·4H$_2$O + CoCl$_2$·6H$_2$O

Fe(CH$_3$COO)$_2$ + Co(CH$_3$COO)$_2$·4H$_2$O

synthesis under N$_2$,
metal salt solutions added to pre-equilibrated
suspension of carbon microparticles,
pH 9.2 by addition of NH$_3$,
equilibration for at 50°C and at 80°C

synthesis under N$_2$,
metal salt solutions added to pre-equilibrated
suspension of carbon microparticles,
pH 9.2 by addition of NaOH,
equilibration for at 50°C and at 80°C

pH 6.5 by addition of NaOH,
ultrasonication for 20 min,
equilibration for 2 days under N$_2$,
solvent evaporation for 20 h at 45°C

Co-precipitation of
Fe and Co oxides on Carbon

Co-precipitation of
Fe and Co oxides on Carbon

Wet impregnation of
Fe and Co acetate salts

drying at 50°C for 12 h,
reduction at 400°C
in N$_2$:H$_2$ 9:1 for 4 h

drying at 50°C for 12 h,
reduction at 500°C
in N$_2$:H$_2$ 9:1 for 4 h

drying at 110°C for 12 h,
reduction in N$_2$:H$_2$ 9:1 in 30 min
steps at 100°C, 300°C, 400°C
and for 2.5 h at 500°C

FeCo on Carbon

FeCo on Carbon

FeCo on Carbon

passivation by 2% O$_2$/N$_2$
for 30 min at 20°C
storage

passivation by 2% O$_2$/N$_2$
for 30 min at 20°C
storage

passivated
FeCo on Carbon

passivated
FeCo on Carbon

passivated
FeCo on Carbon

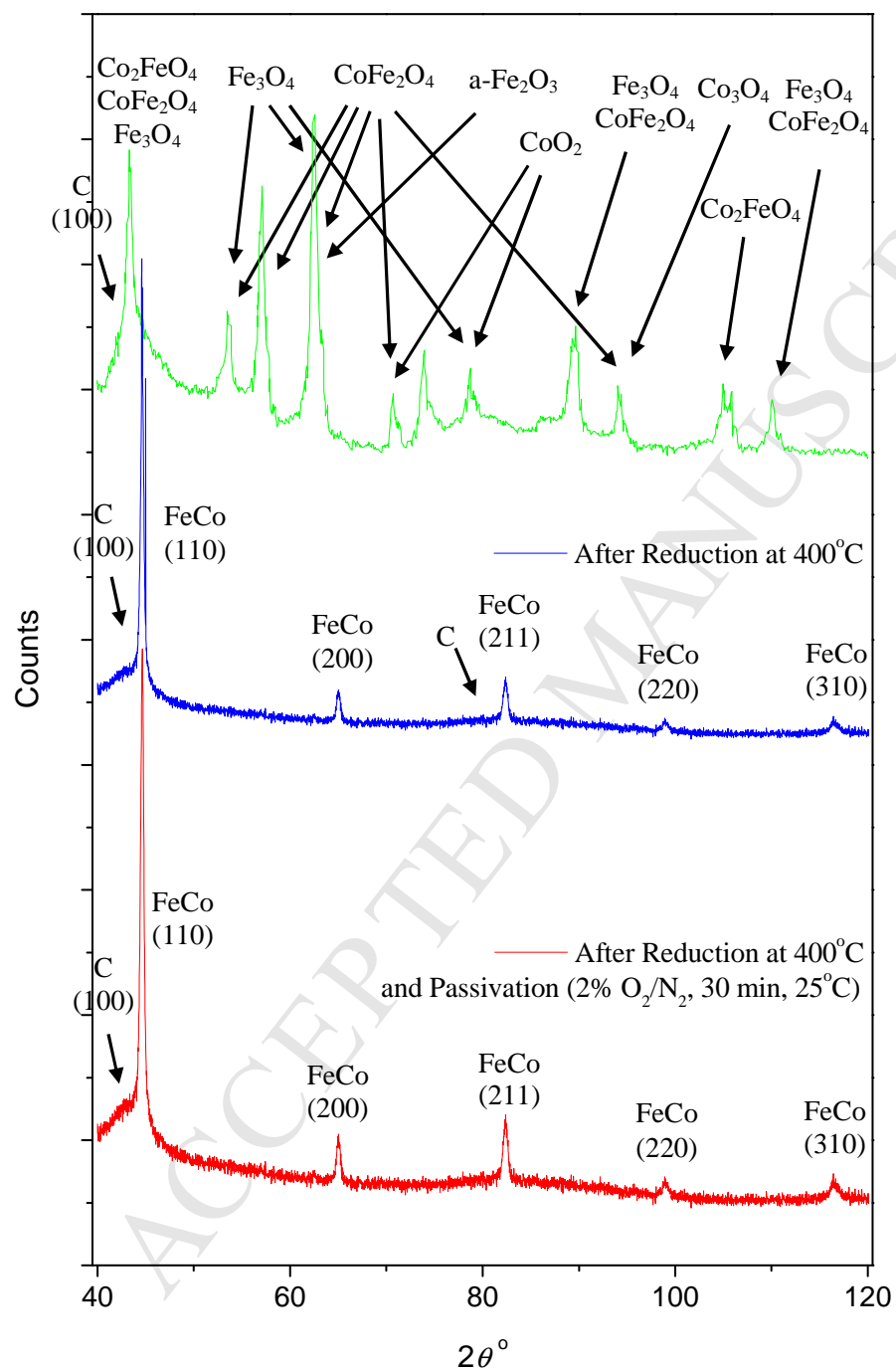Figure 1   Koutsopoulos et al.

Figure 2   Koutsopoulos et al.
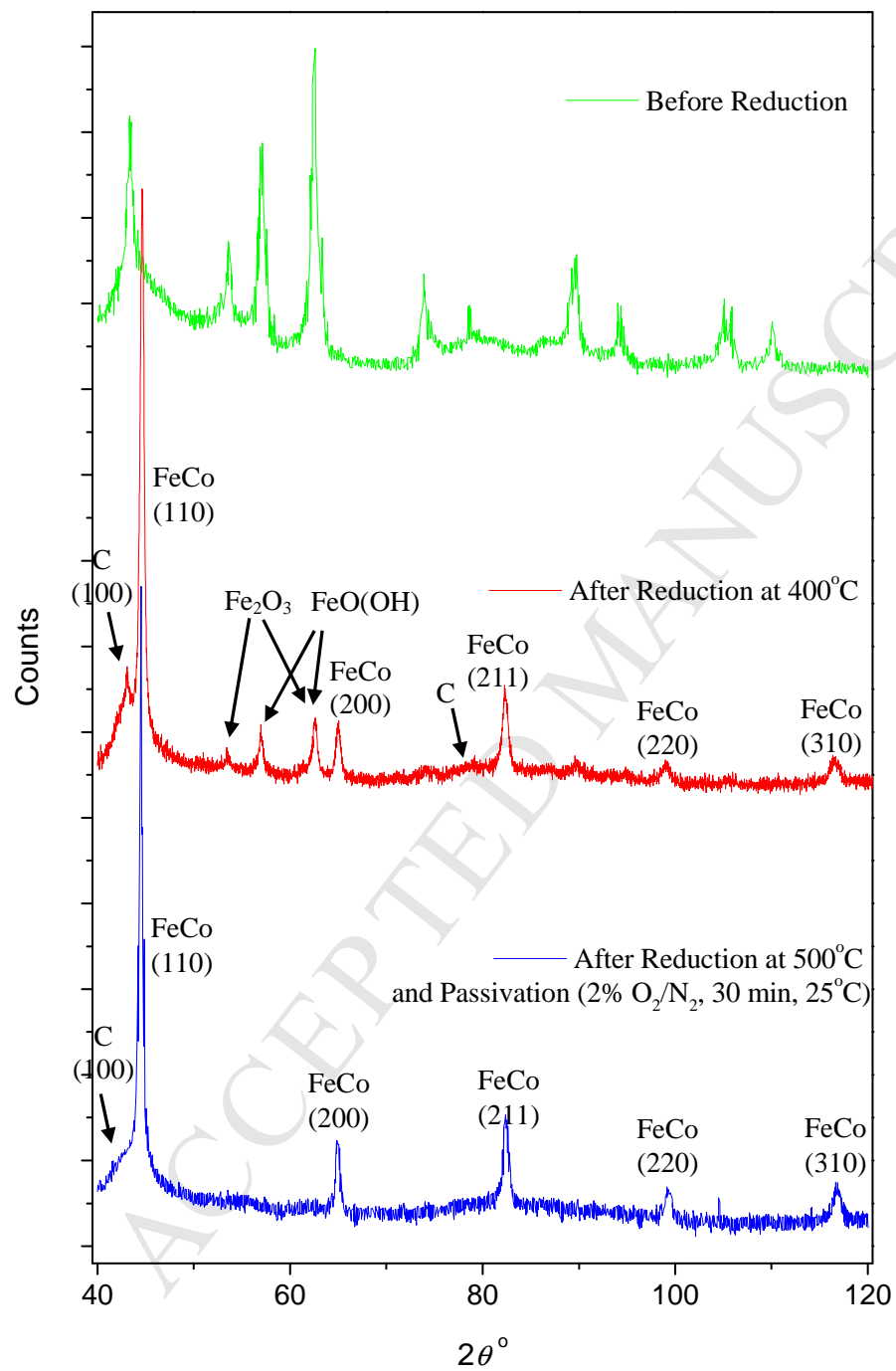
Figure 3   Koutsopoulos et al.
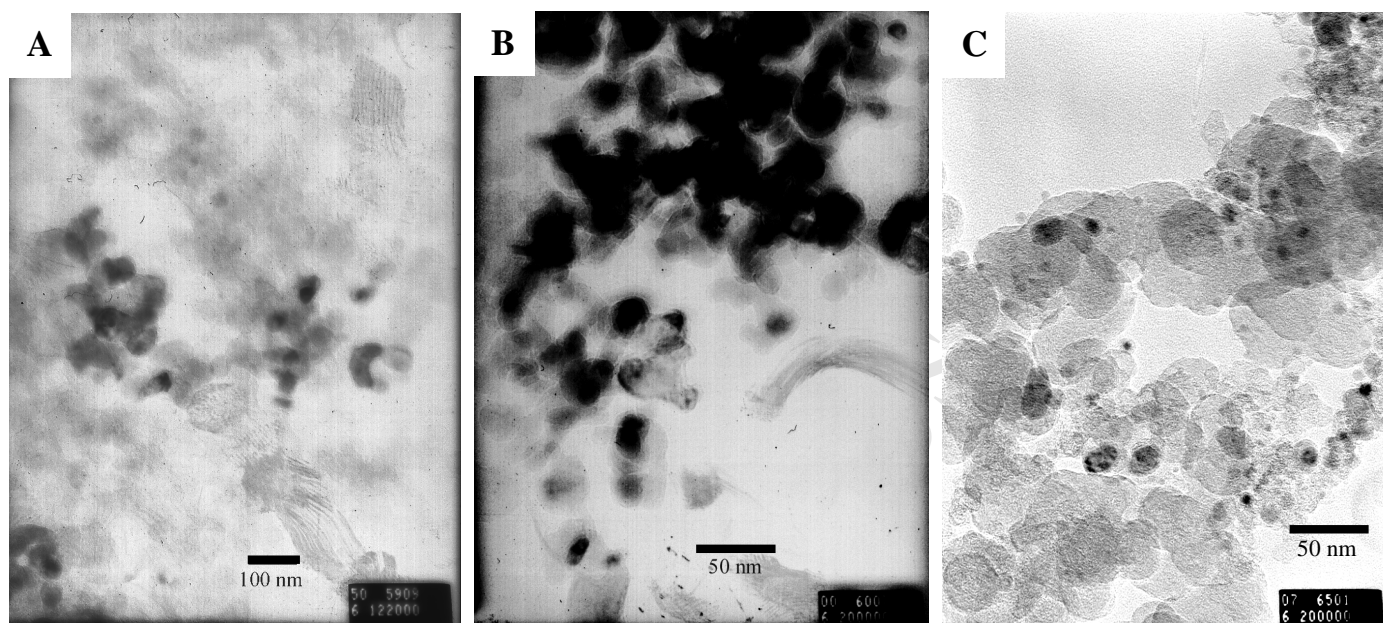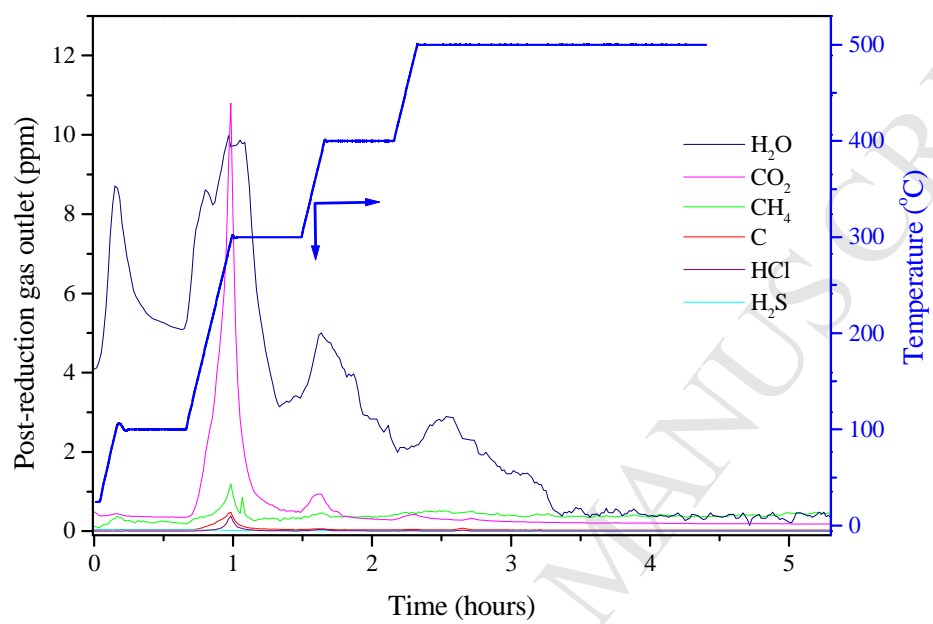
Figure 4   Koutsopoulos et al.

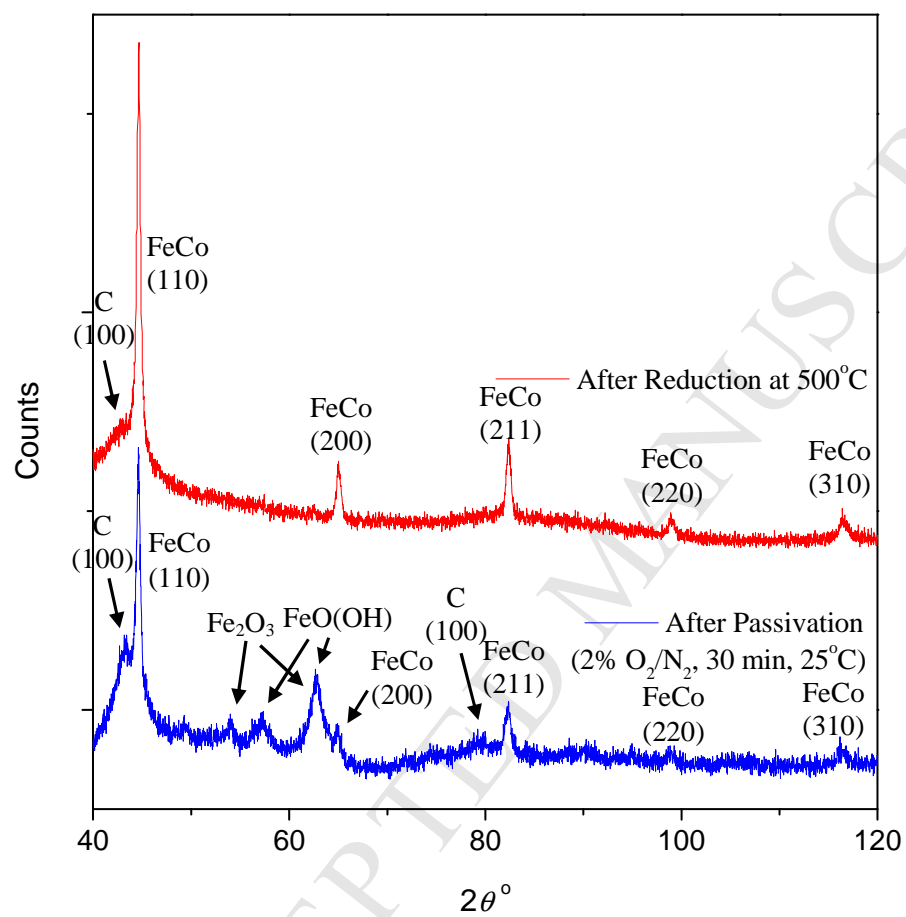Figure 5   Koutsopoulos et al.

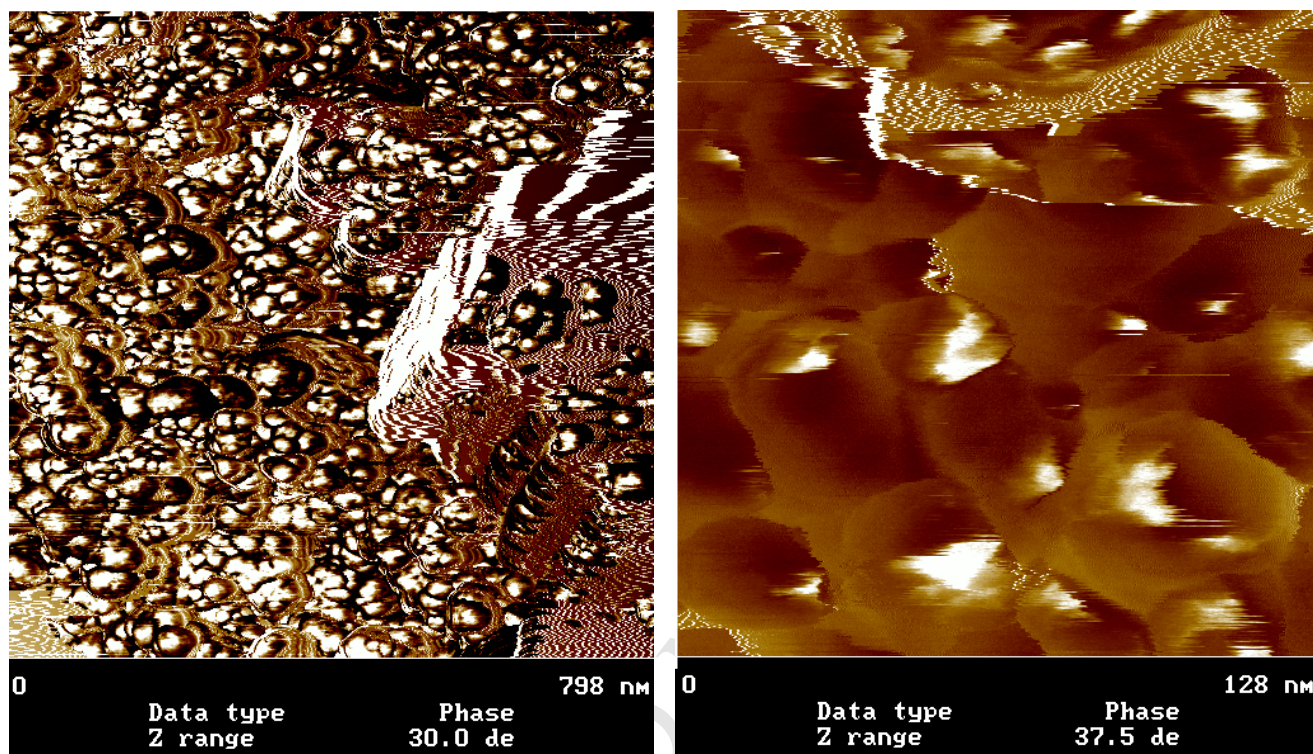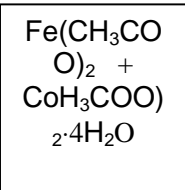Figure 6   Koutsopoulos et al.

Figure 7   Koutsopoulos et al.

Research Highlights

- Synthesis of iron/cobalt alloy nanoparticles supported on carbon microparticles
- Carbon microparticles consist of ~35 nm carbon nanoparticle aggregates
- FeCo alloy and nanoparticles were characterized by XRD, TEM, EDX and AFM
- Co-precipitation of metal oxides results in alloy nanoparticles of 22-24 nm
- Wet impregnation of metal acetates results in alloy nanoparticles of ~13 nm